Nuclear Engineering and Technology 50 (2018) 446–452

Contents lists available at ScienceDirect

Nuclear Engineering and Technology

journal homepage: www.elsevier.com/locate/net

Original Article

Estimation of nuclear heating by delayed gamma rays from radioactive structural materials of HANARO

Tae-yang Noh, Byung-Gun Park*, Myong-Seop Kim

Korea Atomic Energy Research Institute, 111, Daedeok-Daero 989 Beon-Gil, Yuseong-Gu, Daejeon 34057, South Korea

ARTICLE INFO

Article history:
Received 4 August 2017
Received in revised form
8 December 2017
Accepted 8 January 2018
Available online 2 February 2018

Keywords:
Delayed Gamma-ray
HANARO
MCNP
Nuclear Heating
Neutron Irradiation
ORIGEN
Reactor Structure

ABSTRACT

To improve the accuracy and safety of irradiation tests in High flux Advanced Neutron Application ReactOr (HANARO), the nuclear energy deposition rate, which is called nuclear heating, was estimated for an irradiation capsule with an iridium sample in the irradiation hole in order. The gamma rays emitted from the radioisotopes (RIs) of the structural materials such as flow tubes of fuel assemblies and heavy water reflector tank were considered as radiation source. Using the ORIGEN2.1 code, emission rates of delayed gamma rays were calculated in consideration of the activation procedure for 8 years and 2 months of HANARO operation. Calculated emission rates were used as a source term of delayed gamma rays in the MCNP6 code. By using the MCNP code, the nuclear heating rates of the irradiation capsules in the inner core, outer core, and heavy water reflector tank were estimated. Calculated nuclear heating in the inner core, outer core, and heavy water reflector tank were 200–260 mW, 80–100 mW, and 10 mW, respectively.

1. Introduction

Various samples have been irradiated by neutrons at the irradiation holes of High flux Advanced Neutron Application ReactOr (HANARO), a 30-MW multipurpose research reactor of Korea Atomic Energy Research Institute. In these irradiation experiments or tests, various types of radiation are generated, and temperature of the reactor and samples is increased by nuclear heating. Therefore, it is important to ensure in advance that irradiation materials are safe in terms of thermo-hydraulics. To accurately estimate the temperature increase of irradiation materials, detailed analysis of the nuclear heating caused by various types of radiation is required. Nuclear heating in the irradiation material arises from the local deposition of energy carried by neutrons and prompt gamma rays issued from fission, radiative capture and inelastic neutron scattering, and delayed gamma rays emitted by fission and activation product decay. Among these, however, delayed gamma-ray contribution has not so far been estimated in detail at HANARO [1].

It is not easy to experimentally estimate the activities of the radioisotopes (RIs) in structural materials because appropriate measuring methods should be applied for each RI according to the decay type [2]. Furthermore, it is impossible to obtain samples from various locations in the HANARO core. In HANARO, therefore, the Monte Carlo method has been used to correct the delayed gamma contribution to nuclear heating [1]. In this method, the nuclear data library of prompt gamma rays is replaced by the library of delayed gamma rays, and it is assumed that the production rate is the same as the removal rate for all RIs in the structural materials. This method is reasonable if the half-life of the RI is short; otherwise, however, it is not reliable. Other well-known methods to determine the delayed gamma contribution are coupling a Monte Carlo code with an activation analysis code [3] or using the recently developed Monte Carlo codes that contain a built-in module for the activation process [4–6]. In these methods, however, only activation and depletion processes of fuel elements can be considered [4,5]. In addition, tracking of delayed gamma rays after a long-term period of neutron irradiation, for example, several cycles of reactor operation, is not available in the stand-alone Monte Carlo code [6].

In this article, for irradiation capsules that contain an iridium sample, the nuclear heating rates caused by delayed gamma rays (delayed gamma heating) from radioactive structural materials are estimated using Monte Carlo and activation codes. Structural materials near the irradiation capsule are selected as radiation sources, and the activation process of the structural materials is simulated.

* *Corresponding author.*
E-mail address: bgpark@kaeri.re.kr (B.-G. Park).

https://doi.org/10.1016/j.net.2018.01.010

In addition, the emission rates of the delayed gamma rays for each structural material are calculated. The results are presented and discussed in this article. The proposed method can be used in various material irradiation tests in HANARO, and it is expected to improve the reliability of the irradiation tests.

2. Materials and method

2.1. Calculation process

The Monte Carlo particle transport code, MCNP6 [6], and the activation code, ORIGEN2.1 [7], are used to calculate the delayed gamma heating by radioactive structural materials in HANARO. The coupled calculation system using the MCNP and ORIGEN codes is a well-known calculation tool and has been used for various objectives [8–10]. The calculation of the delayed gamma heating is divided into three steps.

In the first step, one-group effective cross-sections for all RIs in the structural materials are calculated using the MCNP code in criticality mode. Among various neutron-induced reactions, (n, γ), (n, 2n), (n, α), and (n, p) cross-sections are considered. The cross-section is calculated using the following formula:

$$\overline{\sigma}_i = \frac{\int \sigma_i(E)\,\phi(E)\,dE}{\int \phi(E)\,dE} = \frac{R^i_{MCNP,1G}/N}{\phi_{MCNP,1G}} \quad (1)$$

where $R^i_{MCNP,1G}$ and $\phi_{MCNP,1G}$ are the one-group reaction rate for RI i and the one-group neutron flux calculated using the MCNP code, respectively. N is the number density of the isotopes, which is calculated from the density and composition of the material. The real neutron flux of the structural material is calculated using

$$\phi_{1G} = \frac{\nu \times P}{\kappa \times k_{eff}} \times \phi_{MCNP,1G} \quad (2)$$

where ϕ_{1G} is the one-group real neutron flux, and ν, P, κ, and k_{eff} are the number of neutron emissions per fission, reactor power, released energy per fission, and effective multiplication factor, respectively. In this study, P and κ were assumed to be 30 MW and 200 MeV/fission, respectively, and ν and k_{eff} were obtained from the MCNP calculation.

In the second step, the emission rates of the delayed gamma rays from the radioactive structural materials are calculated using the ORIGEN code. The one-group effective cross-section in Eq. (1) is used for the nuclear data library of the ORIGEN code, and the one-group neutron flux in Eq. (2) is used for the averaged flux for all the operation cycles. As it is impossible to simulate the real operation cycles of HANARO because of the limitation of the ORIGEN code, pseudo operation cycles are assumed. In the pseudo operation cycles, the number of total cycles is 71, and each cycle has 28 operation days and 14 cooling days. In this operation cycle, the structural materials are irradiated by neutrons for approximately 8 years and 2 months at HANARO. Various types of radiation are emitted with specific energies from the radioactive structural materials during the decay process. The energy distribution and emission probability of the delayed gamma rays are calculated using the ORIGEN code. In the calculation, only delayed gamma rays are considered because alpha rays and beta rays can be negligible owing to their short mean free path. In the ORIGEN code, the energy levels of the emitted gamma rays are collapsed to 18 groups.

In the final step, the delayed gamma heating of the irradiation capsule is calculated using the MCNP code in the fixed source mode. The energy distribution and emission probability of the delayed gamma rays, which are calculated in the second step, are used for the source term of the MCNP calculation.

2.2. Radiation source and target

In the HANARO core, light water enters the core from the lower grid plate and exits to the upper chimney for reactor cooling. Fuel assembly is loaded into the coolant flow tube in the reactor core. The flow tube guides the coolant flow and isolates the coolant from other fuel assemblies or the reflector tank. The reflector tank is filled with heavy water and is separated from the core by the inner shell. Owing to the attenuation of the gamma rays, the delayed gamma heating of the irradiation material is inversely proportional to the square of the distance between the irradiation material and the structural material. Considering the distance from the irradiation capsule, the flow tubes, inner shell, and heavy water were selected as radiation sources in the calculation. These structures are irreplaceable materials and are irradiated for a long time in the core. In the case of the other structural materials, such as the grid plate or the upper chimney, the contribution of delayed gamma heating is negligible because they are located far from the reactor core. The neutron fluxes are small in these structures, and they are irradiated in relatively small amounts. The flow tubes and inner shell are made of Zircaloy-4. The composition of Zircaloy-4 is shown in Table 1.

RI capsules of aluminum alloy with iridium samples were considered as the irradiation material for the calculation of the delayed gamma heating. In the calculation, four sets of RI capsules were loaded into the RI rig. The RI rigs were considered to be loaded at three vertical irradiation holes, Inner Region (IR2), Outer Region (OR6), and Isotope Production (IP11), as shown in Fig. 1. Because neutron flux and energy spectrum are different at the three irradiation holes, delayed gamma heating at various irradiation positions in the core can be considered. The IR2 irradiation hole is located in the inner core where the fast neutron flux is relatively high in comparison with the OR6 and the IP11 irradiation holes, and many flow tubes are installed nearby. In contrast, the OR6 irradiation hole located in the outer core is close to the inner shell; therefore, the epithermal neutron flux is relatively high in comparison with that of the IR2 and the IP11 irradiation holes. The OR6 irradiation hole is directly affected by the flow tubes, inner shell, and heavy water. Meanwhile, the IP11 irradiation hole is located in the reflector tank and far from the fuel; therefore, the total flux in the IP11 irradiation hole is lower than those in the IR2 and the OR6, but the thermal neutron flux is relatively high. Fig. 2 shows side views of the RI capsules in the IR2, OR6, and IP11 irradiation holes. The IR2 hole has a hexagonal shape, but the OR6 and IP11 holes are cylindrical in shape, with the same radius. The RI capsules used for the three different holes are of the same shape.

The neutron flux of the structural materials depends on the position of the structural material. Even in the same structural material, the neutron flux is different depending on the axial and radial directions in the material. To calculate the neutron flux and cross-sections numerically, each structural material was divided into several segments in the calculation model. Each flow tube was divided into four segments in the axial direction, but it is assumed

Table 1
Composition of Zircaloy-4 (density = 6.55 g/cm^3) [11].

Nuclide	Composition	Nuclide	Composition
Zr	98.24%	Sn	1.45%
Fe	0.21%	Cr	0.10%

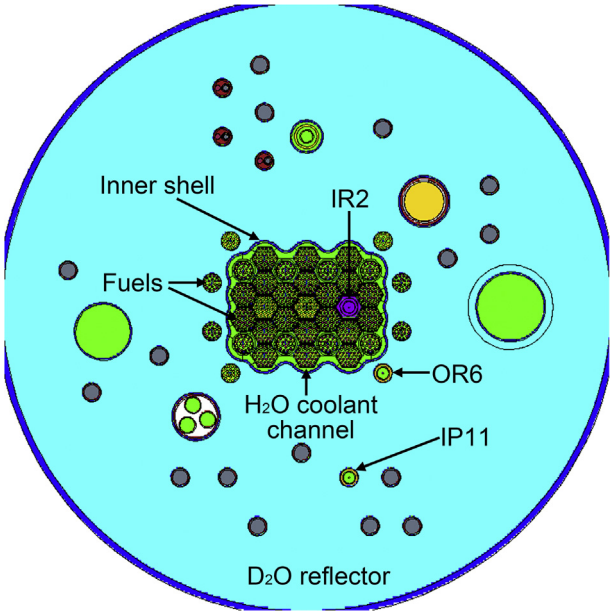

Fig. 1. Locations of the IR2, OR6, and IP11 irradiation holes in the HANARO.
HANARO, High flux Advanced Neutron Application ReactOr; IP, isotope production; IR, inner region; OR, outer region.

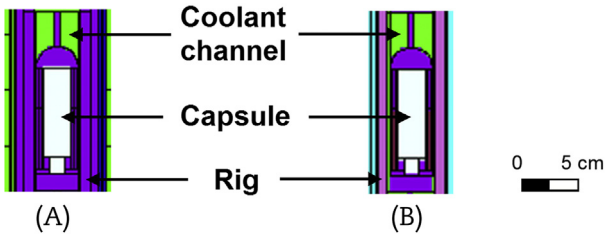

Fig. 2. Vertical view of an RI capsule. (A) For the IR2 irradiation hole. (B) For the OR6 and IP11 irradiation holes.
IP, isotope production; IR, inner region; OR, outer region; RI, radioisotope.

that the neutron flux is uniform in the radial direction. The inner shell was divided into five and 28 segments in the axial and radial directions, respectively. In the case of heavy water, average neutron flux was calculated at the heavy water region.

The probability that the delayed gamma rays reach the RI capsule is inversely proportional to the square of the distance between the structural material and the RI capsule. Therefore, contribution of the delayed gamma rays from structural materials far from the RI capsule can be negligible to the nuclear heating of the RI capsule. Among the structural materials, the heavy water reflector has large volume, and therefore, the radiation source from the heavy water reflector was determined by evaluating the correlation between radial distance from the RI capsule and the heating rates of the RI capsule. To evaluate the heating rate at the OR6 irradiation hole, the heavy water reflector was divided into several concentric circular segments in a radial direction. Fig. 3 shows the accumulated delayed gamma heating of the RI capsules in the OR6 irradiation hole as a function of the radial distance between the RI capsules and the position of the heavy water. As shown in the Fig. 3, the average values of the accumulated delayed gamma heating of four RI capsules at each distance were fitted to an exponential function. The saturated value was calculated to be 0.155 mW, which indicates the nuclear heating at OR6 due to delayed gamma rays in the whole heavy water reflector. The

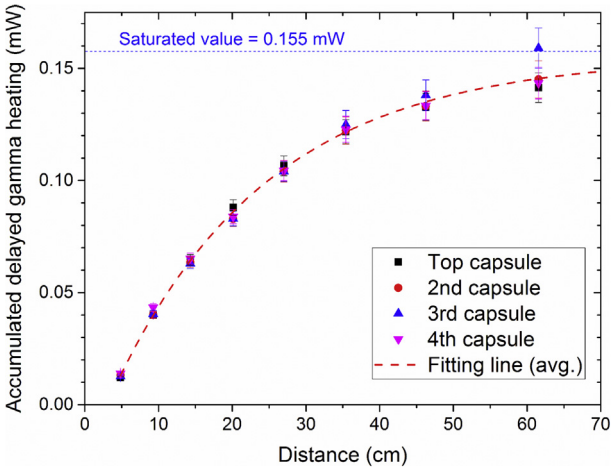

Fig. 3. Accumulated delayed gamma heating of the RI capsules in the OR6 as a function of the radial distance between the RI capsule and a position of the heavy water.
OR, outer region; RI, radioisotope.

radiation source was determined considering a distance of the heavy water reflector from the RI capsule up to 63.8 cm. Although the delayed gamma heating by the heavy water reflector within a distance of 63.8 cm is slightly less than the saturated value, the uncertainty of calculation increases for the greater distance. Therefore, considering a heavy water reflector within 63.8 cm as a radiation source is sufficient for the calculation. Table 2 shows the main RIs of the heavy water and the mean energies and emission rates of the delayed gamma rays from the RIs, which were calculated using the ORIGEN code. Most delayed gamma rays were emitted from N-16, which is produced by the (n, p) reaction of O-16.

In the cases of flow tubes and the inner shell, considering all flow tubes and the whole inner shell as radiation sources is not adequate in consideration of the computing time. Table 3 shows the main RIs of the flow tube (Zircaloy-4) and mean energies and emission rates of the delayed gamma rays from the RIs, which were calculated using the ORIGEN code. The dominant mean energy of the delayed gamma rays from the flow tube is 850 keV, for which the emission rate is 63~87% of the total delayed gamma rays. Because the inner shell is Zircaloy-4, the dominant mean energy of the delayed gamma rays from the inner shell can be assumed to be the same as that from the flow tube. Therefore, the calculation ranges for the flow tubes and inner shell were determined based on the energy absorption coefficient [12,13] of the 850 keV gamma ray in each material. In this study, an energy absorption coefficient of 0.2 is used as a criterion of the calculation range. The flow tubes and part of the inner shell located within the distance corresponding to the criterion were considered as the radiation sources.

Table 2
Emission rates of main gamma rays from the heavy water.

Gamma-ray energy (keV)[a]	Isotope	Emission rate (10^{12} photons/s)
		D_2O reflector
2,750	N-16	0.0373 (1.1%)
7,000	N-16	3.22 (98.5%)
Total[b]		3.27 (100%)

RI, radioisotope.
[a] Mean energy of the main energy group for each RI.
[b] Total emission rate of the gamma rays emitted from all of the radionuclides, including N-16.

Table 3
Emission rates of the main delayed gamma rays from the IR2, OR6, and IP11 flow tubes.

Gamma-ray energy (keV)[a]	Isotope	Emission rate (10^{12} gamma rays/s)		
		IR2 flow tube	OR6 flow tube	IP11 flow tube
575	Nb-97	21.8 (26.2%)	5.21 (17.4%)	0.687 (7.1%)
850	Zr-95	18.6 (22.3%)	9.42 (31.4%)	4.06 (41.7%)
850	Zr-97	15.7 (18.8%)	3.74 (12.5%)	0.493 (5.1%)
850	Nb-95	18.1 (21.7%)	9.13 (30.4%)	3.94 (40.5%)
Total[b]		83.4 (100%)	30.0 (100%)	9.74 (100%)

IP, isotope production; IR, inner region; OR, outer region; RI, radioisotope.
[a] Mean energy of the main energy group for each RI.
[b] Total emission rate of the gamma rays emitted from all of the radionuclides, including Nb-95, 97 and Zr-95, 97.

The radiation sources for the IR2, OR6, and IP11 irradiation holes are depicted in Figs. 4–6, respectively. Considered radiation sources are colored in the figures. For the IR2 irradiation hole, 10 flow tubes for 36 element fuel, four flow tubes for 18 element fuel, two flow tubes for hexagonal irradiation holes, and a half of the inner shell were considered as the radiation sources. For the OR6 hole, three flow tubes for 36 element fuel, three flow tubes for 18 element fuel and a cylindrical irradiation hole, and a quarter of the inner shell were considered. In the case of the IP11 hole, flow tubes for five IP irradiation holes were considered as radiation sources.

3. Results

The calculated delayed gamma heating of the RI capsules in the IR2, OR6, and IP11 irradiation holes are shown in Tables 4–6, respectively. The structures are categorized according to the distance from the RI capsules. The delayed gamma heating rates due to each structure are represented with the statistical errors of the MCNP calculation.

In the case of the IR2 irradiation hole, 94% of the delayed gamma heating is caused by flow tubes. Heating rate due to the inner shell and heavy water is less than 6% of the total delayed gamma heating. Comparing the delayed gamma heating due to a single flow tube, IR2 flow tube is the dominant radiation source. Among the four RI capsules, delayed gamma heating values of the third and fourth RI capsules from the top are higher than those of the other capsules. This is related to the axial distributions of neutron flux of the flow tubes and inner shell. In this study, to simplify the neutron flux and cross-sections used for the activation code, it was assumed that the position of the control rod was 450 mm from the bottom of the core in all operation cycles. In the HANARO operation, control rods are moved rapidly at the beginning of the operation cycle and moved slowly at the middle and end of the operation cycle. In this case, the value 450 mm can be regarded as an average position of the control rod in one operation cycle. As a result, the activities of the lower parts of the flow

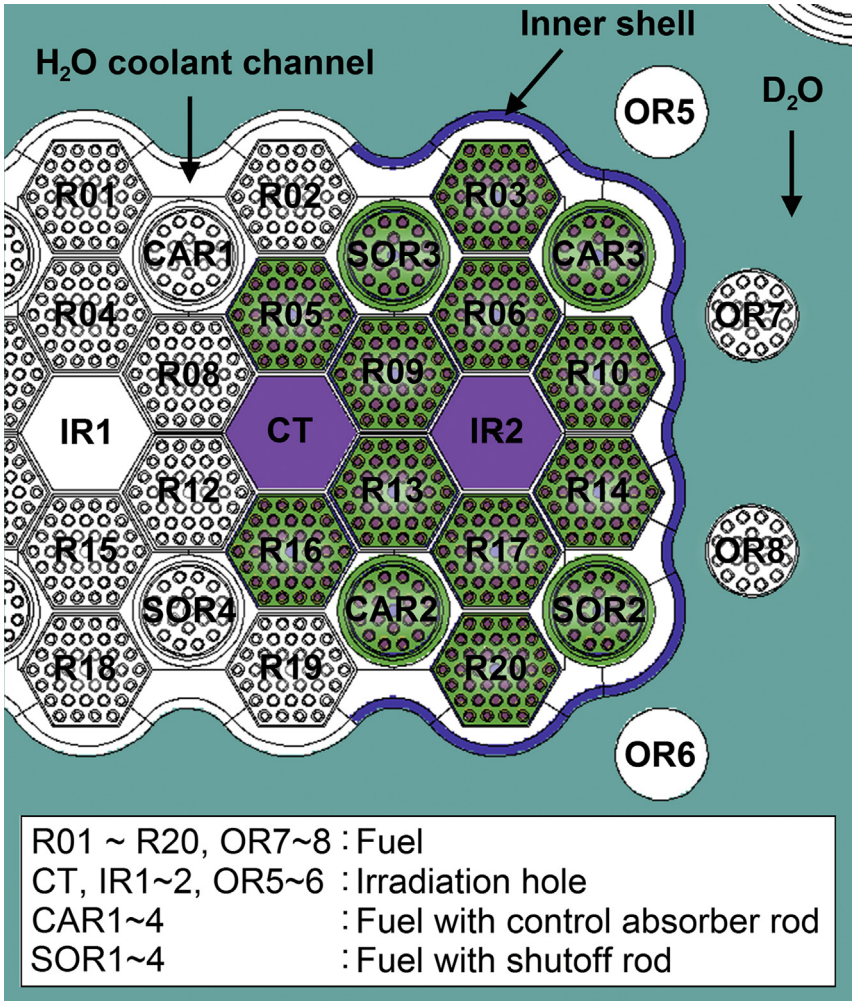

Fig. 4. Considered structural materials as radiation sources for the IR2 irradiation hole.
CAR, control absorber rod; CT, central thimble; IR, inner region; OR, outer region; SOR, shutoff rod.

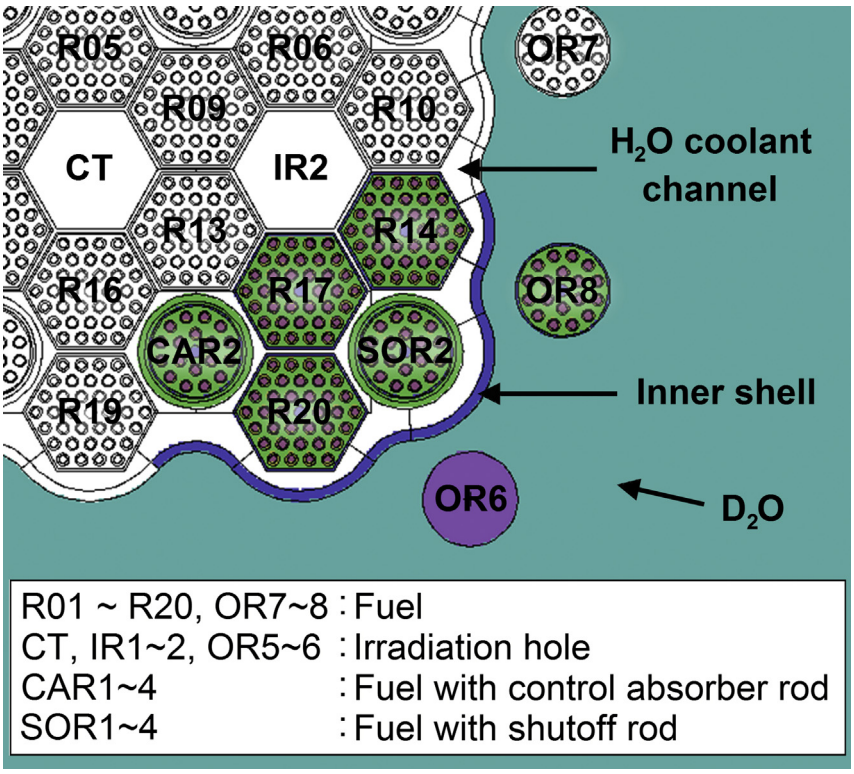

Fig. 5. Considered structural materials as radiation sources for the OR6 irradiation hole.
CAR, control absorber rod; CT, central thimble; IR, inner region; OR, outer region; SOR, shutoff rod.

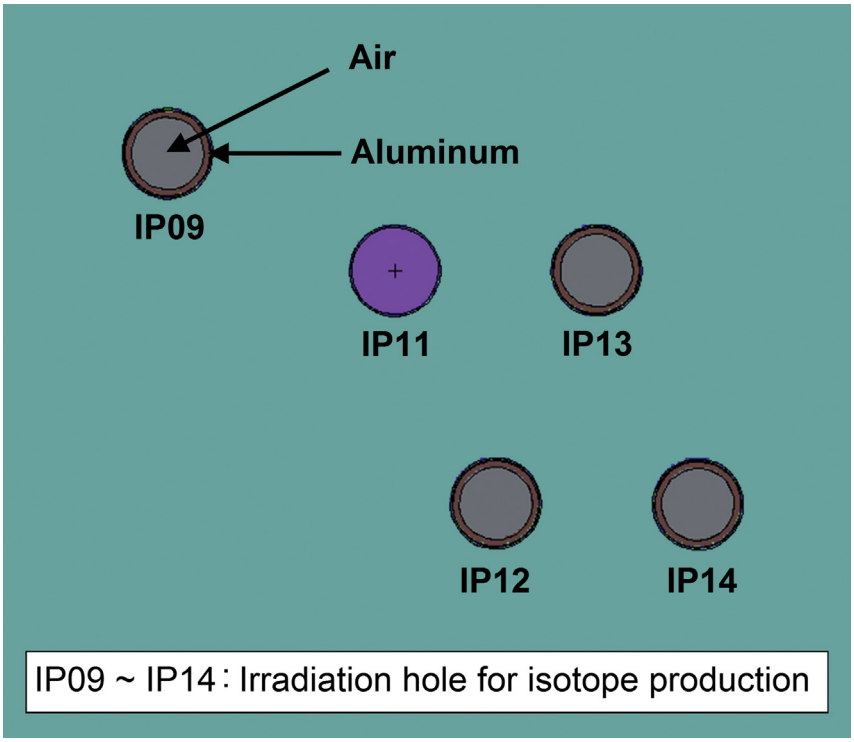

Fig. 6. Considered structural materials as radiation sources for the IP11 irradiation hole.
IP, isotope production.

Table 4
Delayed gamma heating of the RI capsules in the IR2 irradiation hole.

Category of structures	Delayed gamma heating (mW)			
	First capsule	Second capsule	Third capsule	Fourth capsule
IR2 flow tube	42.01 ± 1.69 (24.7%)	48.47 ± 1.81 (27.0%)	60.76 ± 2.02 (24.3%)	56.77 ± 1.98 (25.2%)
R06,09,10,13,14, and 17 flow tubes	69.07 ± 2.41 (40.6%)	68.10 ± 2.37 (37.9%)	95.26 ± 2.79 (38.1%)	87.88 ± 2.67 (39.0%)
R03,05,16,20, and CT flow tubes	46.90 ± 2.20 (27.6%)	46.92 ± 2.17 (26.1%)	70.17 ± 2.76 (28.1%)	61.47 ± 2.56 (27.3%)
CAR2,3, SOR2, and 3 flow tubes	2.89 ± 0.30 (1.7%)	4.11 ± 0.36 (2.3%)	7.25 ± 0.50 (2.9%)	6.09 ± 0.49 (2.7%)
Inner shell	9.10 ± 0.72 (5.4%)	12.17 ± 0.81 (6.8%)	16.33 ± 0.97 (6.5%)	13.29 ± 0.85 (5.9%)
D_2O reflector	0.044 ± 0.006 (0.026%)	0.030 ± 0.005 (0.017%)	0.040 ± 0.006 (0.015%)	0.034 ± 0.005 (0.015%)
Total	170.02 ± 3.76 (100%)	179.80 ± 3.80 (100%)	249.82 ± 4.55 (100%)	225.53 ± 4.31 (100%)

CAR, control absorber rod; IR, inner region; RI, radioisotope; SOR, shutoff rod.

Table 5
Delayed gamma heating of the RI capsules in the OR6 irradiation hole.

Category of structures	Delayed gamma heating (mW)			
	First capsule	Second capsule	Third capsule	Fourth capsule
OR6 flow tube	21.65 ± 0.94 (29.2%)	23.50 ± 0.98 (27.4%)	29.25 ± 1.11 (26.9%)	28.83 ± 1.09 (27.8%)
R20 flow tube	3.83 ± 0.27 (5.2%)	4.13 ± 0.28 (4.8%)	5.00 ± 0.32 (4.6%)	5.12 ± 0.31 (4.9%)
SOR2 flow tube	3.05 ± 0.19 (4.1%)	3.43 ± 0.21 (4.0%)	4.19 ± 0.21 (3.9%)	4.12 ± 0.22 (4.0%)
OR8 flow tube	3.87 ± 0.19 (5.2%)	4.14 ± 0.20 (4.8%)	4.95 ± 0.22 (4.6%)	4.42 ± 0.21 (4.3%)
CAR2 flow tube	0.33 ± 0.06 (0.5%)	0.86 ± 0.12 (1.0%)	1.27 ± 0.14 (1.2%)	1.02 ± 0.11 (1.0%)
R17 flow tube	2.51 ± 0.25 (3.4%)	2.97 ± 0.27 (3.5%)	3.45 ± 0.28 (3.2%)	3.32 ± 0.27 (3.2%)
R14 flow tube	1.94 ± 0.23 (2.6%)	2.47 ± 0.27 (2.9%)	3.94 ± 0.37 (3.6%)	3.40 ± 0.31 (3.3%)
Inner shell	36.77 ± 1.36 (49.6%)	44.12 ± 1.54 (51.4%)	56.49 ± 1.73 (52.0%)	53.47 ± 1.65 (51.5%)
D_2O reflector	0.150 ± 0.007 (0.20%)	0.155 ± 0.009 (0.18%)	0.168 ± 0.009 (0.15%)	0.150 ± 0.007 (0.14%)
Total	74.11 ± 1.73 (100%)	85.77 ± 1.91 (100%)	108.72 ± 2.15 (100%)	103.84 ± 2.07 (100%)

CAR, control absorber rod; OR, outer region; RI, radioisotope; SOR, shutoff rod.

Table 6
Delayed gamma heating of the RI capsules in the IP11 irradiation hole.

Category of structures	Delayed gamma heating (mW)			
	First capsule	Second capsule	Third capsule	Fourth capsule
IP11 flow tube	7.24 ± 0.18 (75.1%)	7.38 ± 0.18 (73.3%)	7.67 ± 0.19 (72.8%)	7.57 ± 0.18 (74.5%)
IP09,12, and 13 flow tubes	1.81 ± 0.10 (18.7%)	2.01 ± 0.11 (20.0%)	2.20 ± 0.12 (20.9%)	1.94 ± 0.11 (19.1%)
IP14 flow tube	0.404 ± 0.015 (4.2%)	0.475 ± 0.017 (4.7%)	0.489 ± 0.017 (4.6%)	0.432 ± 0.016 (4.3%)
D_2O reflector	0.192 ± 0.014 (2.0%)	0.200 ± 0.014 (2.0%)	0.175 ± 0.012 (1.7%)	0.217 ± 0.015 (2.1%)
Total	9.63 ± 0.21 (100%)	10.05 ± 0.21 (100%)	10.53 ± 0.22 (100%)	10.13 ± 0.21 (100%)

IP, isotope production; RI, radioisotope.

tubes and inner shell are higher than those of the upper parts, and therefore, the delayed gamma heating values of the third and fourth RI capsules are relatively high.

Table 5 shows the calculated delayed gamma heating of the RI capsules in the OR6 irradiation hole. The dominant radiation source is the inner shell, which accounts for half of the total delayed gamma heating of the RI capsules. The delayed gamma heating due to the OR6 flow tube, flow tubes of the other assemblies, and heavy water reflector are 30%, 20%, and 0.2% of the total heating rate, respectively. Among the RI capsules, the delayed gamma heating values for the third and fourth RI capsules are relatively high, as in the case of the IR2 irradiation hole.

Table 6 shows the calculated delayed gamma heating of the RI capsules in the IP11 irradiation hole. The IP11 hole is surrounded by heavy water, and a few flow tubes are located around the irradiation hole. The dominant radiation source is the flow tubes. In particular, 74% of the total heating rate is generated by the delayed gamma rays from the IP11 flow tube. The axial distribution of the neutron flux of the IP11 hole is flatter than those in the IR2 or OR6 holes; therefore, the difference in the heating rates among the four RI capsules is relatively less than those in the IR2 or OR6 irradiation holes.

If the neutron energy spectra for all the flow tubes are the same, the emission rate of the delayed gamma rays for each flow tube can be assumed to be proportional to the neutron flux. Therefore, the heating rates of the RI capsules loaded into other irradiation holes can be estimated based on the neutron fluxes of the flow tubes located around each irradiation hole.

The average neutron fluxes of each flow tube in the core are shown in Fig. 7. In the case of the Central Thimble (CT) irradiation hole, the delayed gamma heating of RI capsules due to the R05 flow tube can be estimated by using the results in Table 4, which are the delayed gamma heating values of RI capsules in the IR2 irradiation hole with the R06 flow tube as a radiation source. The heating rates of the RI capsules in other irradiation holes were calculated in a similar manner. In the case of the CT irradiation hole, the average delayed gamma heating of the four RI capsules is 257.46 mW, which was calculated by considering the CT, R02, R04, R05, R06, R08, R09, R12, R13, R15, R16, R17, R19, IR1, IR2, CAR1, CAR2, SOR3, and SOR4 flow tubes. In the case of the OR5, the average delayed gamma heating is 87.66 mW, which was calculated by considering the OR5, OR7, R03, R06, R10, CAR3, and SOR3 flow tubes. In these calculations, it was assumed that the delayed gamma heating resulting from the inner shell and heavy water is the same as the results in Tables 4 and 5.

In the case of the flow tubes at the heavy water reflector tank, the neutron spectra at each flow tube are varied depending on the position because each flow tube is located at a different distance from the reactor core. However, it can be inferred that the delayed

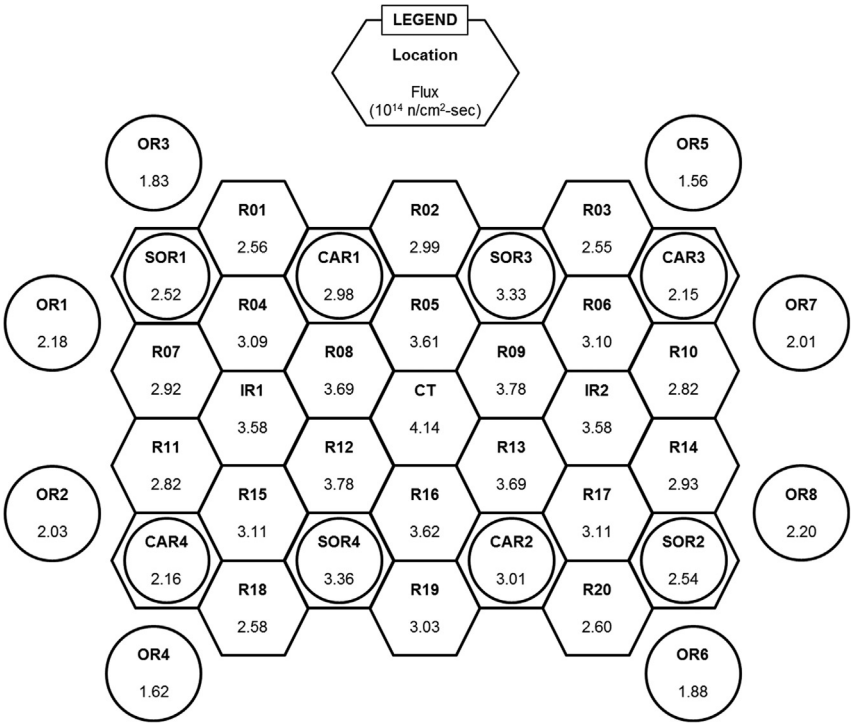

Fig. 7. Locations and averaged fluxes of flow tubes for fuel assemblies in the core of the HANARO.
CAR, control absorber rod; HANARO, High flux Advanced Neutron Application ReactOr; SOR, shutoff rod.

gamma heating rates of the irradiation holes are much lower than those in the core because the structural materials are limited and the neutron fluxes of the structural materials are relatively low.

4. Conclusion and discussion

In this work, the delayed gamma heating rates of RI capsules in the IR2, OR6, and IP11 irradiation holes of HANARO were evaluated. Three irradiation holes were selected by considering the inner core, outer core, and the heavy water reflector tank area of HANARO. For the radiation sources, the delayed gamma rays emitted from the flow tubes, inner shell, and heavy water reflector were considered. The radiation sources were assumed to be irradiated by neutrons over 8 years and 2 months. To calculate the delayed gamma heating due to the flow tubes and inner shell, the range of the radiation source was determined based on the gamma-ray attenuation factor. In the case of the heavy water reflector, the heating rates were estimated using the fitted curve of the accumulated delayed gamma heating as a function of the radial distance from the RI capsules. The average delayed gamma heating rates of four RI capsules in the IR2, OR6, and IP11 irradiation holes were estimated to be 206.29 mW, 93.11 mW, and 10.09 mW, respectively. In all cases, flow tubes near the RI capsules were the dominant radiation sources, and the inner shell is the main radiation source for the OR6 irradiation hole. However, the contribution of the heavy water reflector to the delayed gamma heating was relatively low in all cases.

In general, the delayed gamma heating of the irradiation capsule is relatively less than prompt gamma heating due to the neutron capture reactions in the materials near the irradiation capsule. However, the calculation procedure in this study can be useful for estimation of nuclear heating rates of the irradiation capsule by various types of radiation from other origins, for example, delayed radiations from fission fragments. In the future, by evaluating the levels of nuclear heating rates caused by all radiation sources, the safety of the irradiation capsule will be ensured in terms of thermo-hydraulics, with improved accuracy and reliability.

Conflicts of interest

All authors have no conflicts of interest to declare.

References

[1] B.C. Lee, Analysis on the Detailed Hear Generation Rate for the HANARO, Internal technical report, KAERI/TR-3643/2008, Korea Atomic Energy Research Institute, 2008.
[2] S.B. Hong, B.K. Seo, D.K. Cho, G.H. Jeong, J.K. Moon, A study on the inventory estimation for the activated bioshield concrete of KRR-2, J. Rad. Prot. 37 (Dec. 2012) 202–207.
[3] Y. Chen, U. Fischer, Rigorous MCNP based shutdown dose rate calculations: computational scheme, verification calculations and application to ITER, Fusion Eng. Des. 63–64 (2002) 107–114.
[4] H.J. Shim, C.H. Kim, McCARD User's Manual Version 1.1, Seoul National University, Aug, 2013.
[5] J. Leppanen, Serpent – a Continuous-Energy Monte Carlo Reactor Physics Burnup Calculation Code, VTT Technical Research Centre of Finland, Jun, 2015.
[6] J.T. Goorley, M.R. James, T.E. Booth, MCNP6 User's Manual Version 1.0, LA-CP-13–00634, Rev. 0, Los Alamos National Laboratory, May, 2013.
[7] A.G. Croff, A User's Manual for the ORIGEN2 Computer Code, ORNL/TM-7175, Oak Ridge National Laboratory, 1980.
[8] T. Newton Jr., Z. Xu, M. Kazimi, Modeling the MIT reactor neutronics for LEU conversion studies, in: Proceeding of PHYSOR 2004, Chicago, Apr, 25–29, 2004.
[9] I.C. Gauld, S.M. Bowman, B.D. Murphy, P. Schwalbach, Applications of ORIGEN to spent fuel safetyguards and non-proliferation, in: Proceeding of Institute of Nuclear Materials Management 47th Annular Meeting, Nashville, TN, USA, Jul, 16–20, 2006.
[10] A. Isnaeni, M.S. Aljohani, T.G. Aboalfaraj, S.I. Bhuiyan, Analysis of 99Mo production capacity in uranyl nitrate aqueous homogeneous reactor using ORIGEN and MCNP, J. Atom Indonesia 40 (1) (2014) 40–43.
[11] KAERI/TR-710/1996, Rev. 10, Safety Analysis Report, Korea Atomic Energy Research Institute, Apr, 2017.
[12] J.R. Lamarsh, A.J. Baratta, Introduction to Nuclear Engineering, third ed., Prentice Hall, 2001.
[13] W.G. Unruh, M. Tomlinson, Mean gamma-ray energy absorption coefficients, technical note, Nucl. Appl. 3 (Sep, 1967) 548–549.